

CENTRAL COLLISIONS INDUCED BY LIGHT TARGET NUCLEI

B. M. Badawy

*Reactor Physics Department, Nuclear Research Center, Atomic Energy
Authority, Cairo, Egypt*

E-Mail: badawyfathalla@hotmail.com

Rec. 28/1/2008

Accept. 22/5/2008

For the interactions of p, ^3He , ^4He , and ^6Li with emulsion at 4.5A GeV/c, an experimental study has been performed. The type of interactions chosen was central which enable to analyze a specific interaction mechanism. The selection of the central events has been in the frame work of the particles emitted beyond the kinematic limits ($\theta_{\text{lab}} \geq 90^\circ$). This selection provides a strict criterion to distinguish the central collisions. For the sake of comparison an additional criterion is introduced. It deals with interactions that exhibit an absence of projectile fragmentation. A detailed study of the emitted pions multiplicity is presented. The focusing is on the light emulsion target H and CNO in comparison with the heavy AgBr. The analysis reveals that, the occultation of light projectile nuclei is possible in CNO targets along with the complete occultation in AgBr.

Keywords: *Central collisions of light projectile nuclei with emulsion, centrality criteria, (H, CNO, and AgBr targets).*

INTRODUCTION

At high energy (say Dubna energy), it is very important to learn as much as possible about all the phenomena which occur in the interactions of nuclei. This should make easier the observation of the anticipated signatures of phase transition to quark – gluon plasma on the background of "normal phenomena".

In study of nucleon – nucleus and particularly nucleus – nucleus collisions it is customary to divide the physics to be studied into two broad categories corresponding to peripheral and central collisions. Nuclear collisions with small impact parameters, i.e. (central) collisions, are of interest for a study of nuclei in extreme states. Central

collisions give rise to a large range of complex phenomenon that can result in the catastrophic destruction of the interacting nuclei. In central collisions the maximum possible number of participating nucleons from the overlapping region between the target and projectile takes part in the interaction. Therefore, it becomes possible to study the characteristics of interactions which are definitely many nucleon interactions.

Because central collisions at high energies subject nuclear matter to physical conditions heretofore unavailable in the laboratory, there is much theoretical and experimental activity on this aspect of high energy physics [1 – 24].

From the methodological and theoretical standpoints the collisions of two identical nuclei are the most convenient for state. The symmetry in the initial state makes it possible to determine the center –of– mass (c. m) frame, which in this case is the same as the c. m frame for nucleon – nucleon interactions at the same momentum per nucleon.

In the present work, the central collisions of light projectiles (p, ^3He , ^4He , and ^6Li) relatively near compared with light emulsion target, which consists of H, C, N, and O nuclides, have been investigated. One of the principal objectives of this experiment was to discover whether or not the interactions with light nuclei (H, CNO) at high energy, selected on the basis that, the collisions were central, or near central, show phenomena significantly different from that observed in previous experiments [3, 6, 12, 14, 17, 22, 23] involving heavy targets (AgBr).

Finally, central collisions may be considered the most appropriate for studying the highly excited and compressed hadronic matter and the quark – gluon plasma [15].

EXPERIMENTAL DETAILS

Emulsion and Exposures

The Dubna energy (a few GeV/A) is a special energy, at which the nuclear limiting fragmentation applies initially [25]. Hence, the NIKFI–BR2 nuclear emulsion stacks measured in this experiment were exposed by p, ^3He , ^4He , and ^6Li beams at the Synchrophasotron (JINR), Dubna, Russia. The beams momentum is $4.5A$ GeV/c. Each emulsion pellicle size is 10 cm x 20 cm x 600 μm . Table 1 shows the chemical composition of this emulsion type. This table gives the density corresponding to each element of the emulsion constituent in atoma/cm³ [26].

Table 1. The chemical composition of NIKFI–BR2 emulsion.

Element	^1H	^{12}C	^{14}N	^{16}O	^{80}Br	^{108}Ag
Atoms /cm ³ x 10 ⁻²²	3.150	1.410	0.395	0.956	1.028	1.028

Reaction Mean Free Path

Starting close to the entrance of the beam into the emulsion (0.5 cm) along-the-track, double scanning; fast in the forward and slow in the backward direction; was carried out. The total scanned lengths (L) of primary beam tracks, the number of resulted inelastic interactions (N), and the corresponding average values of experimental mean free path (λ) for different projectiles are listed in Table 2.

Table 2. Beams interactions data for different projectiles.

Projectile	L m	N Events	λ cm
p	799.998	2649	30.20±0.70
³ He	332.600	1685	19.74±0.48
⁴ He	217.600	1092	19.93±0.60
⁶ Li	148.450	1019	14.57±0.46

Identification Methods

Depending on ionization, all tracks emitted from the interaction vertices were classified according to the commonly accepted emulsion experiment terminology [27] as:

- 1) Shower particles – tracks with $g \leq 1.5g_p$. They mainly, consist of pions having energy above 70 MeV and singly charged particles with energy above 400 MeV. Their multiplicity is denoted as n_s . The multiplicity of shower particles emitted in the forward hemisphere (FHS) ($\theta_{lab} < 90^\circ$) is denoted as n_s^f . The multiplicity of shower particles emitted in the backward hemisphere (BHS) ($\theta_{lab} \geq 90^\circ$) is denoted as n_s^b .
- 2) Grey particles – tracks with $1.5g_p < g < 4.5g_p$; they consist mainly of protons knocked – out from the target nucleus during the collision with a few percent admixture of π mesons. Their multiplicity is denoted as N_g .
- 3) Black particles – tracks with $g > 4.5g_p$, mostly protons. Their multiplicity is denoted as N_b .

Here, g is the measured grain density and g_p corresponds to the grain density of a minimum ionizing track. Grey and black tracks amount the group of heavily ionizing tracks $N_h = N_g + N_b$.

- 4) Fragments of projectile nucleus with $Z \geq 1$, the projectile fragments PF's essentially travel with the same speed as that of the parent beam nucleus, so the energy of the produced PF's is high enough to distinguish them easily from the target fragments. All PF's are emitted in a very narrow forward direction ($\theta_{lab} \leq 3^\circ$) within an angle given by the Fermi momentum. PF's with $Z = 1$ and 2 are identified by visual inspection of tracks where, their ionizations are similar to those of shower and grey particles, respectively.

DEMONSTRATIVE SURVEY

Impact Parameter

The impact parameter, b of a nucleus – nucleus collision is classically defined by the distance between the straight line trajectories of the centers of the two nuclei before their interaction. The impact parameter is not directly measurable. It is thus necessary to find an observable strongly correlated with it.

The simplest observable one can think of is the multiplicity of target fragments, N_h . This parameter was used widely by the many authors [8, 16, 28, 29] for presenting their results.

In an inelastic collision of a relativistic nucleus, not all the nucleons of the incident nucleus actually interact with the target nucleus. Some of the nucleons remain spectators or "stripping" nucleons, as they are frequently called. The interaction of nuclei heavier than the deuteron the stripping particles may include not only nucleons but also larger fragments of the projectile nuclei in the form of stable and radioactive elements. The stripping particles lie in narrow momentum and angular intervals because of the Fermi motion of the nucleons in the projectile nucleus. All particles with $Z \geq 1$ and rapidity, (the Lorentz invariant parallel velocity) above half the beam rapidity, are regarded as projectile fragments of charge Z_{pf} . Therefore, in order to classify the events with respect to the actual impact parameter, the parameter $Q = \sum Z_{pf}$, was introduced, [3, 6, 16, 17].

Target Separation and Inelastic Interactions Cross Section

Nuclear emulsion is a composite medium composed of H, CNO, and AgBr. It is a difficult task to separate interactions on different classes of targets. Although there are many correlations between the measured parameters that give information regarding the target nuclei, it is impossible to find certain separation criteria that give no admixture between those classes.

Depending upon the target break-up, one uses the heavily ionizing particles multiplicity N_h as a parameter representing the impact parameter in experiment. Hence, the N_h – integral distribution method described explicitly in refs. [28–30] is used to select from the inelastic interactions samples those with hydrogen H, light CNO, and heavy AgBr targets. According to this method all events with $N_h > 8$ are considered to be due to interactions with AgBr group. The events with $N_h \leq 8$ are attributed to interactions with the H, CNO, and peripheral collisions with AgBr.

The experimental cross sections belonging to each target group of interactions σ_H , σ_{CNO} , σ_{Em} , and σ_{AgBr} are computed as, $\sigma = \frac{1}{\lambda\rho}$ [29, 30]. Here, λ is substituted as

the measured mean free path of the projectile interactions with each target group and ρ is the density of that group of nuclei given in Table 1. Accordingly, the deduced values of the cross sections due to the inelastic interactions of p, ^3He , ^4He , and ^6Li (4.5A GeV/c) with emulsion and its target groups are listed in Table 3.

Table 3. The experimental values of inelastic cross section of each projectile with different emulsion targets at 4.5A GeV/c together with their corresponding empirical predictions.

Projectile	σ_H mb	σ_{CNO} mb	σ_{Em} mb	σ_{AgBr} mb
p	37.70±3.87 (32.3)	291.36±11.50 (249.79)	415.52±8.07 (357.03)	1161.37±26.58 (998.67)
³ He	89.72±9.25 (84.10)	527.05±23.96 (489.77)	635.70±15.49 (591.76)	1618.57±48.65 (1506.62)
⁴ He	100.67±12.13 (103.42)	533.89±29.79 (546.64)	629.64±19.05 (644.54)	1568.97±59.21 (1605.15)
⁶ Li	162.53±18.64 (138.42)	755.74±42.94 (641.52)	861.26±26.98 (732.51)	2074.12±82.44 (1765.00)

On the other hand, the inelastic cross section is predicted empirically from a phenomenological "hard-sphere" model using "Bradt – Peters" formula [31]. For projectile nuclei at different incident energies up to 200A GeV, EMU01 collaboration [32] had deduced the cross section formula as,

$$\sigma_{PT} = 109.2(A_p^{0.29} + A_T^{0.29} - 1.39)^2 \text{ mb} \quad (1)$$

The empirical predictions of the cross section according to formula (1) are given in Table 3 between parentheses.

The Picture of Central Collisions

In the picture of a "hadron – hadron" collisions, the projectile and the target are spatially extended objects. In the region of violent collision they hit each other so hard that they arrest each other and form a conglomerate which expands and then decays when a critical volume is reached [2]. A high energy nucleus – nucleus collision can be considered as the simultaneous collision between all possible pairs of effective targets and effective projectiles. Therefore, the collision between an effective target and an effective projectile can also be described by the same picture as that used to describe the collision between two hadrons [2]. A nucleus – nucleus reaction is said to be a violent collision process if all or almost all the possible pairs of effective projectile – effective target process are violent [2]. In violent processes the colliding objects lose their identity after the collision. The produced particles are emitted from a compound system formed by the two colliding objects. The relatively large energy and momentum transfers in such reactions manifest themselves in producing particles with large transverse momentum and/or in creating more particles in that collision events [4].

Near-central collisions, lead to a high energy fragments distributed over most of the forward hemisphere with no clear – cut distributions as to their emission from target or projectile [1]. In addition to these fragments, and to pions created in the reaction, there is a low energy component observed in these violent processes which is isotropically distributed over 4π . It may be attributed to decays of a target remnant that did not witness the violent primary interactions [1]. Streamer chamber experiments at

high incident energy [1] reveal overall multiplicities of charged particles that are high, reaching up to the total number of initial charges plus a significant number of created charged pions. This high multiplicity indicates that an almost complete dissociation of both target and projectile is an event frequently associated with near-central impact. It had been generally accepted that a high multiplicity of fragments and pions at large angles and intermediate energies may be used as a distinctive feature that allows one to select near-central collisions of relativistic nuclei. These nonperipheral but not necessarily head-on collisions will henceforth be called central collisions [1].

Two extreme concepts of the mechanism for the fast stage in a central collision are a superposition of nucleonic cascade or the formation of an intermediate or quasi-equilibrated system. In the former case the observable decay features would result from well-known nucleon-nucleon cross sections folded with initial target and projectile ground state single particle distributions [1].

Central collisions of nuclei at relativistic energies were predicted by dynamical models [7] to proceed via a compression-expansion cycle of the participating hadronic matter. In a central Ca + Ca collision at 2A GeV, Stock [7] expected that the pion multiplicity is a steep function of the beam energy over a wide domain, rendering that probe sensitive to the detail of the reaction mechanism up to several GeV/A. The hydrodynamical model was used as one developed, which describes the evolution of the central rapidity region formed in a central collision [9]. The dynamical evolution of central collisions induced by GeV light-ion projectiles was examined with two different Boltzmann-Uehling-Uhlenbeck (BUU) calculations [13]. The behavior of hot heavy residues formed in central collision between light-ion projectiles and heavy target nuclei changes markedly as the beam energy increases from 1 to 10 GeV [13]. A decrease in the number of target fragments with increasing centrality was observed for interactions of projectiles with masses comparable or greater than the mass of the target nucleus [18]. As the collision becomes more central a significant number of participating protons from the target nucleus get enough momentum to become relativistic due to intranuclear interactions [18].

Centrality Criteria

From straight forward geometrical considerations, central collisions are corresponding to the collisions with the impact parameters $0 \approx b \leq |R_T - R_P|$, where R_T and R_P are the radii of target and projectile nuclei respectively.

Exactly, there is no strict definition of what is meant by central collisions. To find the physical quantities that are sensitive to the centrality in nucleon-nucleus and nucleus-nucleus collisions at high energy, it is important to understand the behavior of the very hot and dense nuclear matter formed in these collisions.

Hence, Heckman et al [3] defined the more central collisions as interactions that exhibit an absence of projectile fragments i.e., $Q = 0$. This criterion is also used in experiments [6, 17].

The second approach of centrality estimation is based on the multiplicity of the target fragments N_h . That criterion is used in [6, 8, 16].

The pion multiplicity may be also used in the selection of central collisions [8, 10, 16, 18, 23].

The most central collisions are selected by momentum tensor elongation and multiplicity criteria [11, 12] where the centrality selection is based on the primary charged particle multiplicity N_{ch} [19, 20, 21, 24].

Poisson Distribution

Gyulassy and Kauffmann [33] showed that a broad range of thermodynamic models predicts a Poisson distribution in the emitted pion multiplicity in the central collision. In heavy ion – collision physics, a lot of activity has been devoted to studying of the pion multiplicity distribution in order to find any deviation from Poisson distribution given by expression (2), corresponding to the estimated mean multiplicities $\langle n_i \rangle$.

$$P(n_i) = \frac{\langle n_i \rangle^i}{n_i!} \cdot e^{-\langle n_i \rangle} \quad (2)$$

However, no deviation was found [10].

Hagedorn Spectrum

In the statistical thermodynamic model for the strong interactions, Hagedorn combined statistical thermodynamic features and relativistic kinematics to get results which explained the different characteristics (multiplicity, angular, and momentum distributions) of the multiparticle production at incident energy less than 40A GeV [34]. The expression (3) was obtained by Hagedorn [34], corresponding to the estimated mean multiplicities $\langle n_i \rangle$.

$$P(n_i) = n_i^{3/2} \cdot e^{\frac{-n_i}{0.4\langle n_i \rangle}} \quad (3)$$

RESULTS AND DISCUSSION

It has become customary to consider the process of high energy hadron – nucleus and nucleus – nucleus interactions as a two stage process. The first stage is characterized by a time scale of the order of the light traversal time through the nucleus. In this stage multiparticle production takes place leaving the colliding nuclei in highly excited states. After a relatively long time, the second stage, i.e., the de-excitation of the nuclear remnants starts, manifested by the emission of fragments [18]. In this manner, experimental evidences for the present picture in the case of hadron – nucleus processes have been given in p – Em interactions. The nucleus – nucleus are given in ^3He , ^4He , and ^6Li interactions with emulsion. The dependence on the incident momentum is not a parameter here, where the momentum is the same (4.5A GeV/c).

Selection of Centrality Criteria

In central collisions the projectile and the target nuclei suffer an almost head – on collision. As a result, the target nucleus is left in a highly excited state, which subsequently evaporates [8]. On the other hand, in free nucleon – nucleon collisions, the hadron emission in the BHS is kinematically restricted. The study of hadron emission beyond the kinematic limits ($\theta_{lab} \geq 90^\circ$) in nucleus – nucleus collisions reveals signatures for a collective mechanism recognizing such emission. Therefore, it was concluded that [29 , 30], the backward particle production is a consequence of a decay of a highly excited target system after the forward particle emission. This backward production is mainly dependent on the target. It was also shown that [35 , 36], the dependence of backward hadrons emission on $n_s^b > 0$ is nearly equivalent to the dependence on $Q = 0$. Thus, n_s^b can be used as an indication to the degree of violence of the collision [35 , 36]. Throughout the interactions of ^{12}C , ^{22}Ne , and ^{28}Si with emulsion at Dubna energy, El-Nadi et al [14] argued that, n_s^b is strongly correlated with N_h . This means that, the number of created shower particles in the BHS is a target dependent parameter. Thus, n_s^b was introduced as a new centrality parameter associated with the target source achieving the violent interactions at its higher values [14 , 22].

Results on mean multiplicities of backward showed particles are listed in Table 4. One shows that, $\langle n_s^b \rangle$ values for all projectiles are equal within experimental error at fixed target. For light targets (H, CNO) the values of $\langle n_s^b \rangle$ are equal. For heavy target AgBr, the values of $\langle n_s^b \rangle$ are greater than those for light targets where the target source effect is clear.

The present study pertains to shower particles that are primarily associated with target ($n_s^b > 0$). Another selected criterion adopted to define a collision as "central" here, is that it exhibits an absence of projectile fragmentation ($Q = 0$).

Table 4. The average shower particle multiplicities $\langle n_s^b \rangle$ in the BHS through the interactions with different emulsion targets at 4.5A GeV/c.

Target	H	CNO	AgBr
p	0.16±0.02	0.16±0.01	0.27±0.01
^3He	0.14±0.02	0.14±0.01	0.36±0.01
^4He	0.17±0.02	0.17±0.01	0.44±0.02
^6Li	0.16±0.02	0.16±0.01	0.56±0.02

For proton interactions the criterion $Q = 0$ is not applicable where the incident charge $Z = 1$. Therefore, the most adequate selection to consider the task for proton collisions is $n_s^b > 0$.

Characteristics of Central Collisions

To study the interaction mechanisms of central collisions one may look at the multiplicities of the produced pions per event [4].

Figures 1, 2, 3, and 4 exhibit the normalized multiplicity distributions of the shower particles emitted in the FHS. The data are catalogued according to $n_s^b > 0$ [closed squares] and $Q = 0$ [opened squares]. Two parametric representations of the multiplicity distributions have had particularly widespread usage; the Poisson distribution and Hagedorn spectrum. Drawn through the data are curves derived from the fitted Poisson distributions (solid curves) and Hagedorn spectra (dashed curves).

In Figure 1. an almost symmetric peaking is observed in the central collision of protons with H target. In the central collisions of protons with CNO and AgBr a sideward peaking is observed. The distributions for CNO and AgBr show a steep fall off with increasing multiplicity followed by a fast declining tail at highest multiplicity, regarding to the longer tail for AgBr. The complete diving of the proton into the heavier target nuclear matter results in high multiplicity reflected to central collisions [5]. Angelov et al [37] found that, at a comparatively low primary momentum ($P_0 \sim 4$ GeV/c) there can be essentially no more than one inelastic collision of the primary proton with nucleons of the nucleus leading to the production of pions. Consequently, the increase in the number of collisions with nucleons in the "more central" collisions with nuclei causes an increase in the yield of backward protons, dose not have any significant effect on the average pion multiplicity. The Poisson shapes are superimposed with the data. Their peak positions exhibit the same value of $n_s^f \approx 1.5$ for all states. The Hagedorn spectra can adequately describe the data. As a trend such spectra seem to be slightly steeper than Poissonic ones with the same peak positions.

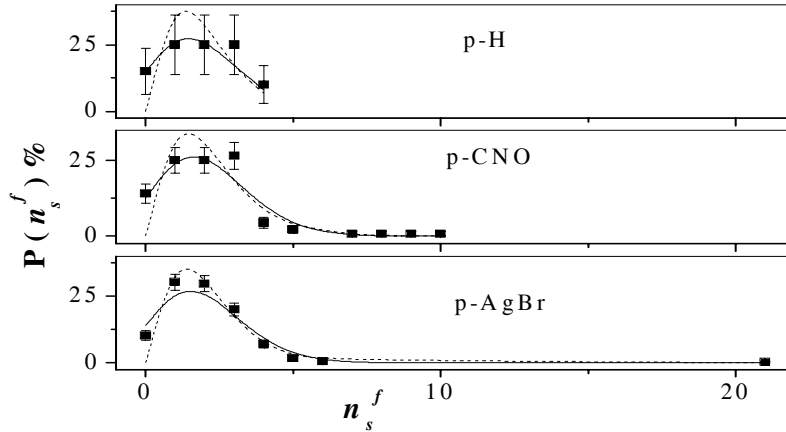


Figure 1. The forward shower particles multiplicity distributions in the interactions of proton with H, CNO, and AgBr at $n_s^b > 0$, together with the corresponding Poisson shapes (solid curves) and the Hagedorn spectrum (dashed curves).

An extended range of the distribution for heavier beams compared with the proton case may be understood in terms of a larger number of collisions between the

nucleons of the interacting nuclei. Therefore, Figure 2. shows the multiplicity distributions of shower particles emitted in the FHS through the central collisions of ${}^3\text{He}$ with different emulsion targets. In the collision of ${}^3\text{He}$ with light targets H and CNO the distributions show structure similar to the proton data, but with peaks shifted forward. The curves have pronounced peaks centered around $n_s^f \approx 4$ ($Q = 0$) and $n_s^f \approx 3$ ($n_s^b > 0$). A shift towards higher values of the peaks for the heavy target AgBr is clearly displayed. The data are reproduced well by the two parametric distributions used (Poisson and Hagedorn).

From Figure 3 one can notice that the curves for ${}^4\text{He}$ central collisions induced by H, CNO, and AgBr as one similar to those for ${}^3\text{He}$.

Presented in Figure 4 are the results on the forward shower particles multiplicity distributions of ${}^6\text{Li}$ interactions with H, CNO, and AgBr. The data are selected for both voted centrality criteria. As can be seen the data could be reasonably well represented by Poisson distributions. The peaking for central collisions induced by the light targets H and CNO is similar, while it shifts forward for AgBr. The peak position as obtained from Poisson fits is steeper than that from Hagedorn fits.

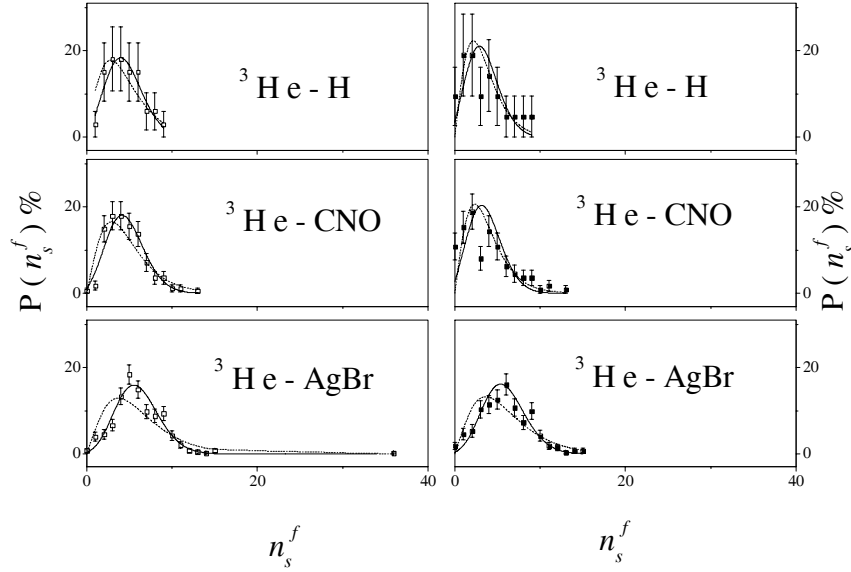


Figure 2. The forward shower particles multiplicity distributions in the interactions of ${}^3\text{He}$ with H, CNO, and AgBr at $Q = 0$ (opened squares), and $n_s^b > 0$ (closed squares), together with the corresponding Poisson shapes (solid curves) and the Hagedorn spectrum (dashed curves).

The principal features characterizing the previous distributions are;

- No observed dependence on replacing one selected centrality criterion by the other is found.
- For all used projectiles the central collisions exhibit a universal trend of peaking.

– All the distributions are Poissonic.

Fragments from central collisions of relativistic heavy ions may originate from several qualitatively different subsystems of the overall decaying nuclear system, such as the fireball, the target spectators, or alternatively, an explosion of the fused target – projectile system [1]. Hence, the Hagedorn spectrum evidences that it can be used to describe the central collisions yields. However, one can observe a sideward shift in such spectrum to the left of the Poissonic ones in nucleus – nucleus central collisions. This shift is more appreciable in the collisions induced by heavier targets.

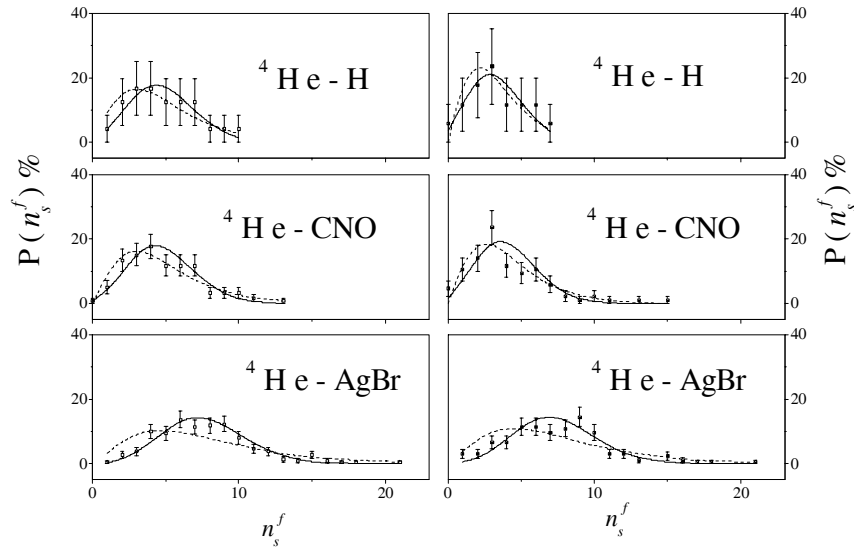


Figure 3. The forward shower particles multiplicity distributions in the interactions of ${}^4\text{He}$ with H, CNO, and AgBr at $Q = 0$ (opened squares), and $n_s^b > 0$ (closed squares), together with the corresponding Poisson shapes (solid curves) and the Hagedorn spectrum (dashed curves).

- For all targets, the shapes of distributions are almost insensitive to the choice of projectile.
- The common feature of the central collisions induced by light targets is that, the peak positions of the distributions for H are never strongly deviating from those of CNO.
- At high energies, mainly the central, symmetric collisions have possibilities to exhibit a one source topology due to the rapid separation of participants and spectators, after which exchange of mass, momentum and energy vanishes [5]. Central collisions of equal–size nuclei are dominated by the formation and decay of a fireball system [5]. Therefore, the almost symmetrical distributions observed here are those of H targets. Their natures look like those of peripheral collisions.
- Unlike the hydrogen targets, for the central collisions induced by CNO the distributions show a slight trend of suppression of forward emission or even a sideward peaking is observed. Central collisions of light projectiles with heavy targets exhibit an

enhancement in sideward emission which was predicted by realistic hydro dynamical model [5]. The tail of distributions representing the suppressions seem to grow with increase of the projectile mass. Such a shape has a very clear interpretation if one recalls central collisions. Therefore, the used projectiles can be occulted in CNO showing the observed peaks. This response of the nuclear medium is a witness of the occurrence of central collisions with CNO targets.

– Regarding to the larger size of AgBr, the figures manifest a similar picture as that of CNO with a systematic peak positions shift towards higher multiplicities of n_s^f than CNO. This confirms the strong signs of central collisions induce by AgBr where a complete occultation of projectiles in the target is expected.

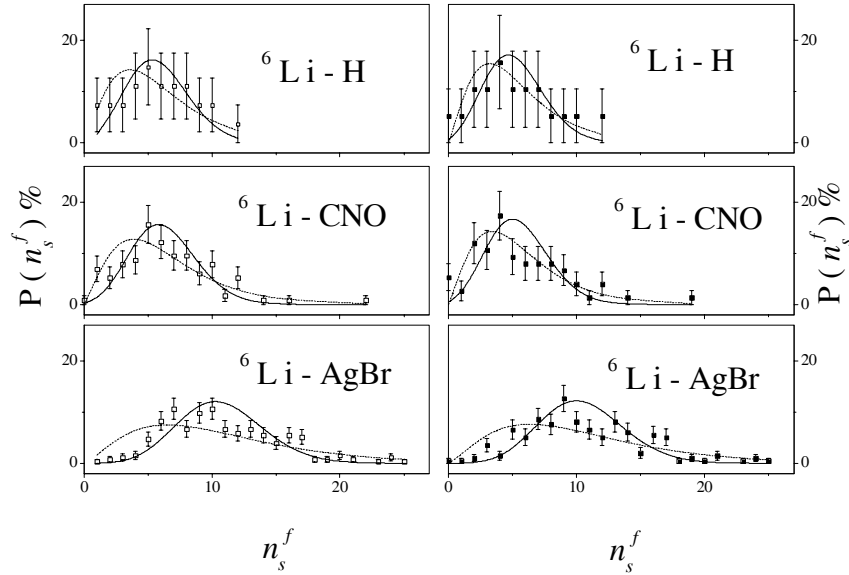


Figure 4. The forward shower particles multiplicity distributions in the interactions of ${}^6\text{Li}$ with H, CNO, and AgBr at $Q = 0$ (opened squares), and $n_s^b > 0$ (closed squares), together with the corresponding Poisson shapes (solid curves) and the Hagedorn spectrum (dashed curves).

These results are similar to that observed by Heckman et al. [3]. They [3] attributed the low-prong number peak to collisions between the ${}^4\text{He}$ projectile and CNO, and the high-number peak to collisions with AgBr because He can be occulted in CNO as well as in AgBr collisions. The absence of CNO peak in the ${}^{16}\text{O}$ and ${}^{40}\text{Ar}$ [3] prong distributions indicated that, non-occultation of the projectile by the target nucleus occurring in collisions between those heavy projectile nuclei and light CNO targets invariably shows evidence for projectile fragmentation.

The results on the mean multiplicities are listed in Table 5. The table includes also the average numbers of shower particles $\langle n_s^f \rangle$ emitted in the FHS through the interactions of p, ${}^3\text{He}$, ${}^4\text{He}$, and ${}^6\text{Li}$ with different emulsion targets at 4.5A GeV/c. The

average values comprise the data base where the associated centrality selections were applied beside the total sample for each target. From Table 5 one can observe the clear increase in $\langle n_s^f \rangle$ with projectile mass number. For central collisions induced by a specific target, the values of $\langle n_s^f \rangle$ are nearly equal under both centrality selections. The values of $\langle n_s^f \rangle$ for the central collisions induced by AgBr are greater than those of H and CNO. The values of $\langle n_s^f \rangle$ for central collisions with H and CNO are similar. These observations confirm what were investigated in Figures 1– 4. It can be shown that, each value of $\langle n_s^f \rangle$ agrees well with the peak positions associated with the distributions in Figure 1– 4. It can be also shown that, the ratio of $\langle n_s^f \rangle_{\text{central}} / \langle n_s^f \rangle_{\text{total}} \approx 1.7$ for $Q = 0$. This value corresponds to the interaction of any projectile with any target. The same trend is observed for $n_s^b > 0$ criteria where $\langle n_s^f \rangle_{\text{central}} / \langle n_s^f \rangle_{\text{total}} \approx 1.4$. These ratios are less than those obtained for $^{16}\text{O} - ^{207}\text{Pb}$ interactions at 200A GeV/c [38]. It was found that [38], the average multiplicity comes from central collisions is three times higher than the mean multiplicity of all the events. This difference is due to the higher incident energy and the size of the colliding nuclei in the experiment of [38]. Central collisions of nearly equal – mass nuclei seem to create a composite system moving with the fireball rapidity [5]. On heavy nuclei, however, central collisions seem to form a highly excited system that is moving relatively slowly in the laboratory frame. This effect indicates a transverse spreading of the incident energy across the heavy target nucleus, to a degree much higher than is implied by the geometrical localization assumed in the fireball model. The projectile does not sweep out a fireball but appear rather to be stopped inside the target matter [5].

Data obtained for light nuclei, and for minimum bias trigger conditions are close given from Wroblewski – relation, $D = \langle n_s \rangle$, characterizing hadron – hadron collisions, where D is the dispersion of the multiplicity distributions [7 and references therein]. Central trigger data approximate the Poisson relation $D^2 = \langle n_s \rangle$ [7 and references therein].

For the present experimental results, the dispersion D of the shower particles emitted in the FHS is plotted as a function of the average multiplicity in Figures 5 and 6. The dispersion D is defined as,

$$D = \sqrt{\langle (n_s^f)^2 \rangle - \langle n_s^f \rangle^2} \quad (4)$$

In Figures 5. and 6. the results are performed for the two criteria selections ($n_s^b > 0$ and $Q = 0$), respectively. As can be seen in the three insets of Figures 5 and 6, straight lines are obtained irrespective of target. As A_p increases, the dispersion increases rapidly with $\sqrt{\langle n_s^f \rangle}$. A straight line fit to the three sets of central interactions induced by H, CNO, and AgBr were calculated. The linear relation fitting the data has the form,

$$D = A + B \cdot \sqrt{\langle n_s^f \rangle} \quad (5)$$

The values of A and B for the two centrality solutions are given in Table 6.

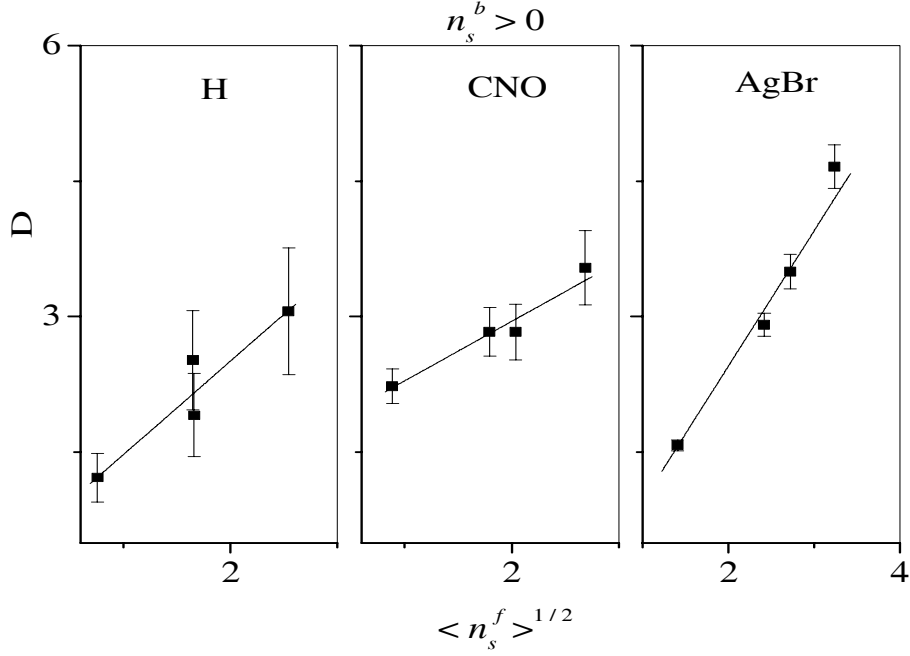


Figure 5. The dispersion of forward shower particles distributions versus $\sqrt{\langle n_s^f \rangle}$ in the interactions of p, ^3He , ^4He , and ^6Li with different emulsion targets at $n_s^b > 0$, together with the linear fitting of the experimental results.

Table 6. Characteristics of linear fits correlating D with $\sqrt{\langle n_s^f \rangle}$ using the two centrality selections.

Target	A(Q=0)	A($n_s^b > 0$)	B(Q=0)	B($n_s^b > 0$)
H	-4.17 ± 0.62	-1.63 ± 0.71	2.93 ± 0.28	2.07 ± 0.43
CNO	-5.15 ± 1.09	0.32 ± 0.30	3.46 ± 0.49	1.32 ± 0.17
AgBr	-1.70 ± 0.72	-0.53 ± 0.23	1.86 ± 0.27	1.49 ± 0.13

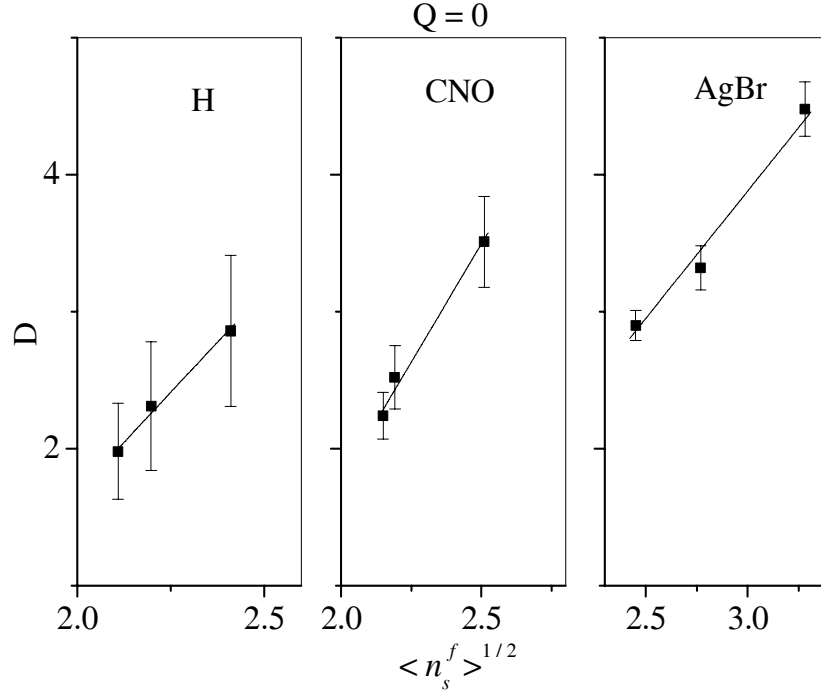


Figure 6. The dispersion of forward shower particles distributions versus $\sqrt{\langle n_s^f \rangle}$ in the interactions of p, ^3He , ^4He , and ^6Li with different emulsion targets at $Q = 0$, together with the linear fitting of experimental results.

Since the behavior is the same for the three targets, one can say that the change of D with the produced multiplicity is independent of the size of the interacting system at fixed momentum. The linear dependence expected from a Poisson distribution is generally observed irrespective of the applied centrality criteria. Observations similar to this had been reported in Refs. [10, 39, 40], where another selection of centrality criteria was applied.

Cross Sectional Observations

The cross sections here, are the probabilities that an ion with a given charge, mass and energy interacts with a given target nucleus producing central collision events.

Table 7 presents the cross sectional values σ of the central collisions induced by H, CNO, and AgBr at 4.5A GeV/c. The calculations of σ values are executed as detailed through the demonstrative survey and categorized as the two associated centrality criteria. From Table 7 one can notice that, the cross sectional values increase

gradually with the projectile mass number A_p . The increase of σ values with the target size is fast. Therefore, the dependence on the target size is strong.

Table 8 gives the ratios of the cross sectional values associated with the centrality criterion ($Q = 0$) to those with ($n_s^b > 0$). Within error, the ratios seem to have the same value ≈ 1.4 . Therefore, each one of centrality parameters can scale well to the other achieving a constant value. One can say that, the selection of central collision events using any one of the mentioned criteria reveals a constant trend irrespective of projectile and target combinations.

The cross sectional values associated with the selectivity of ($Q = 0$) could be correlated with ($n_s^b > 0$) in Figure 7. The data of all targets seem as if they are locating on one straight line. In Figure 7., each line segment fitting the experimental data has a slope value close to unity for the three targets. This reflects the asymptotic behavior of using the selected criteria for central collisions.

Finally, Table 9 includes the relative values of the induced central collision cross sections [given in Table 7] to the total inelastic cross sectional values [given in Table 3]. From Table 9 one can observe that, the ratios belonging to $Q = 0$ for the three targets $\approx 35\%$, while those for $n_s^b > 0$ are having ratios $\approx 23\%$. The experimental study using different projectiles at high energy reported by Angelov et al.[39]. They found that, the number of central collisions turned out to constitute a fraction $\approx 24\%$ of all inelastic CTA interactions. Through a study of $^{16}\text{O} - ^{207}\text{Pb}$ collisions at 200A GeV/c in the frame work of the dual parton model, Capella et al [38] showed that, approximately one of each five events comes from central collisions. In p – nucleus interactions at 0.8 and 1.6 GeV [10], it was shown that, central collisions will be taken towards the highest multiplicity representing about 20 % of the geometrical cross section. In Au – Em interactions at 10.7A GeV, Adamovich et al [16] found that, the central samples $\approx 25\%$ of the total sample. Therefore, in despite of the dissimilarity or similarity among the interacting systems of the present work and the others [10 , 16 , 38 , 39], the common result is that; "The central collisions induced by a specific target establish about [20 % – 25 %] of the total sample with this target". Moreover, the selection of the centrality parameters in this work demonstrates a good agreement with the others [10 , 16 , 38, 39]. Such agreement was more distinct in applying n_s^b than Q.

Table 8. The ratios between the central collisions cross sections corresponding to $Q = 0$ and those corresponding to $n_s^b > 0$ at different emulsion targets.

Target	H	CNO	AgBr
^3He	1.57±0.51	1.51±0.21	1.43±0.13
^4He	1.44±0.50	1.41±0.22	1.30±0.14
^6Li	1.40±0.45	1.55±0.26	1.30±0.13

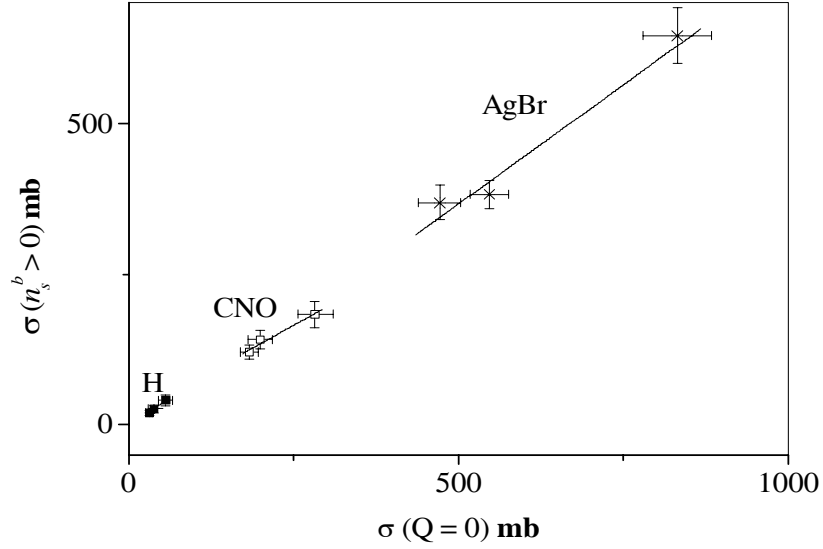


Figure 7. The central collisions cross sectional values corresponding to $n_s^b > 0$ versus those corresponding to $Q = 0$ in the interactions of ${}^3\text{He}$, ${}^4\text{He}$, and ${}^6\text{Li}$ with different emulsion targets, together with the linear fitting of experimental results.

Table 9. The ratios between the central collisions cross sections and the total cross section of each emulsion target in percent according to the two centrality criteria.

Projectile	$\sigma_{\text{H}}(\text{central})/\sigma_{\text{H}}(\text{total})$		$\sigma_{\text{CNO}}(\text{central})/\sigma_{\text{CNO}}(\text{total})$		$\sigma_{\text{AgBr}}(\text{central})/\sigma_{\text{AgBr}}(\text{total})$	
	$Q = 0$	$n_s^b > 0$	$Q = 0$	$n_s^b > 0$	$Q = 0$	$n_s^b > 0$
p	–	21.06 ± 0.05	–	21.13 ± 0.02	–	17.80 ± 0.10
${}^3\text{He}$	35.11 ± 0.06	22.34 ± 0.05	34.71 ± 0.03	22.93 ± 0.02	33.79 ± 0.02	23.58 ± 0.01
${}^4\text{He}$	37.68 ± 0.08	26.09 ± 0.06	37.41 ± 0.04	26.50 ± 0.03	30.06 ± 0.02	23.51 ± 0.02
${}^6\text{Li}$	34.21 ± 0.07	25.00 ± 0.06	37.45 ± 0.04	24.21 ± 0.03	40.13 ± 0.03	31.12 ± 0.02

Table 5. The average shower particle multiplicities in the FHS at $Q = 0$, $n_s^b > 0$, and the total sample through the interactions with different emulsion targets at 4.5A GeV/c.

Target	H			CNO			AgBr		
Projectile	Q = 0	$n_s^b > 0$	Total Sample	Q = 0	$n_s^b > 0$	Total Sample	Q = 0	$n_s^b > 0$	Total Sample
p	–	1.90±0.43	1.71±0.18	–	2.08±0.18	1.78±0.07	–	1.97±0.09	1.88±0.04
³ He	4.45±0.78	3.33±0.73	2.59±0.27	4.62±0.36	3.60±0.34	2.65±0.12	6.01±0.16	5.84±0.18	4.20±0.13
⁴ He	4.83±0.99	3.35±0.81	2.99±0.36	4.80±0.44	4.07±0.31	3.02±0.17	7.67±0.23	7.41±0.27	4.83±0.18
⁶ Li	5.81±1.12	5.16±1.18	3.42±0.39	6.30±0.59	5.49±0.63	3.60±0.20	10.75±0.28	10.49±0.33	5.26±0.21

Table 7. The central collisions cross sections with different emulsion targets at 4.5A GeV/c using the two centrality criteria.

Projectile	σ_H mb		σ_{CNO} mb		σ_{AgBr} mb	
	Q = 0	$n_s^b > 0$	Q = 0	$n_s^b > 0$	Q = 0	$n_s^b > 0$
p	–	7.94±1.78	–	61.57±5.28	–	206.71±11.21
³ He	31.50±5.49	20.04±4.38	182.95±14.12	120.87±11.47	546.92±28.28	381.68±23.62
⁴ He	37.93±7.44	26.26±6.19	199.74±18.24	141.48±15.34	471.63±32.46	368.81±28.70
⁶ Li	55.60±10.90	40.63±9.32	283.00±26.28	182.99±21.13	832.27±52.21	645.45±45.97

CONCLUSION

The central events extracted from the interactions of p, ^3He , ^4He , and ^6Li with emulsion at 4.5A GeV/c have been analyzed. From the analysis one can conclude:

- The n_s^b parameter for selecting central collisions shows the same strong selectivity for critical collisions as Q.
- The forward shower particle distributions for centrally selected events could be reasonably well represented by Poisson distributions.
- The description of the multiplicity distribution by Hagedorn spectra is limited and seen to be relevant for sharply defined centrality.
- The suppression of forward emission in central CNO and AgBr targets collisions is systematically shift of the sideward yield. The data might be understood in terms of a realistic hydro dynamical model as a collective and dispersive sideward flow of matter initiated early in the collision, during penetration [5]. This would also explain why one does not observe the same phenomenon in collisions of nuclei with similar mass. This effect indicates that, the origin of the observed phenomenon is not of a simple kinematic nature.
- The results evidence the possibility of central collisions of light projectile nuclei by CNO targets as near as AgBr.
- A transverse spreading of the incident energy across the heavy target nucleus yields a higher average multiplicity of pions in the forward direction.
- The data approximate the Poisson relation $D\alpha\sqrt{n_s^f}$ for central collisions induced by all targets.
- The central collisions represent about [20 % – 25 %] of the total inelastic interactions, irrespective of the colliding system or the applied centrality criteria.

ACKNOWLEDGEMENTS

The author appreciates the guidance and advice given by Prof. Dr. A. Abdelsalm, the head of Mohamed El-Nadi high energy Lab., at Cairo University, where this work has been carried out. I wish to acknowledge the staff of high energy lab. at JINR, Dubna, Russia for supplying the irradiated emulsion plates.

REFERENCES

- [1] Gosset, J., Gutbrod, H.H., Meyer, W.G., Poskanzer, A.M., Sandoval, A., Stock, R., and Westfall, G.D., *Phys. Rev. C* **16**, 629(1977).
- [2] Mathis, H.B., and Meng Ta-chung, *Phys. Rev. C* **18**, 952(1978).
- [3] Heckman, H.H., Crawford, H.J., Greiner, D.E., Lindstrom, P.J., and Lance W. Wilson, *Phys. Rev. C* **17**, 1651(1978).

- [4] Meng Ta–chung, *Phys. Rev. Lett.* **42**, 1331(1979).
- [5] Stock, R., Gutbrod, H.H., Meyer, W.G., Poskanzer, A.M., Sandoval, A., Gosset, J., King, C.H., King, G., Lukner, Ch., Nguyen Van Sen, Westfall, G.D., and Wolf, K.L., *Phys. Rev. Lett.* **44**, 1243(1980).
- [6] Abdelsalam, A., Vokál, S., Tolstov, K.D., Shabratova, G.S., Šumbera, M., Haiduc, M., Bogdanov, S.D., Ostroumov, V.I., Bogdanov, V.G., Plyushchev, V.A., Solovieva, Z.I., and Togoo, R., *Czech. J. Phys.* **B34**, 1196(1984).
- [7] Stock, R., *Physics Reports* **135**, 259(1986).
- [8] Jain, P.L., Sengupta, K., and Singh, G., *Phys. Rev. Lett.* **59**, 2531(1987).
- [9] ean–Yves Ollitrault, *Phys. Lett.* **B273**, 31(1991).
- [10] Lemaire, M.,–C., et al., *Phys. Rev.* **C43**, 2711(1991).
- [11] Barz, H.W., Bondorf, J.P., Donangelo, R., Hansen, F.S., Jakobsson, B., Karlsson, L., Nifenecker, H., Elmér, R., Schulz, H., Schussler, F., Sneppen, K., and Söderström, K., *Nucl. Phys.* **A548**, 427(1992).
- [12] Schussler, F., Nifenecker, H., Jakobsson, B., Kopljar, V., Söderström, K., Leray, S., Ngô, C., Souza, S., Bondorf, J.P., and Sneppen, K., *Nucl. Phys.* **A584**, 704 (1995).
- [13] Wang, G., Kwiatkowski, K., Viola, V.E., Bauer, W., and Danielewicz, P., *Phys. Rev.* **C53**, 1811 (1996).
- [14] El–Nadi, M., Ali–Mossa, N., and Abdelsalam, A., *IL Nuovo Cimento* **A110**, 1255(1998).
- [15] Pshenichnov, I.A., Mishustin, I.N., Bondorf, J.P., Botvina, A.S., and Iljinov, A.S., *Phys. Rev.* **C57**, 1920(1998).
- [16] Adamovich, M.I., et al., *Eur. Phys. J.* **A1**, 77(1998).
- [17] El–Nadi, M., El–Nagdy, M.S., Abdelsalam, A., Shaat, E.A., Ali–Mossa, N., Abou–Moussa, Z., Abdel–Waged, Kh., Abdalla, A.M., and El–Falaky, E., *Eur. Phys. J.* **A10**, 177(2001).
- [18] Dąbrowska, A., Holyński, R., Olszewski, A., Szarska, M., Trzupek, A., Wilczyńska, B., Wilczyński, H., Wolter, W., Wosiek, B., and Woźniak, K., *Nucl. Phys.* **A693**, 777(2001).
- [19] Adcox, K., et al., *Phys. Rev. Lett.* **86**, 3500(2001).
- [20] Adler, C., et al., *Phys. Rev. Lett.* **89**, 202301(2002).
- [21] Adams, J., et al., *Phys. Rev. Lett.* **91**, 172302(2003).
- [22] Rashed, N., *Arab Journal of Nuclear Sciences and Applications* **37**, 217(2004).
- [23] Vrláková, J., Vokál, S., and Dirner, A., *Acta Physica Slovaca* **56**, 83 (2006).
- [24] Back, B.B., et al., *Phys. Rev.* **C74**, 021902(R) (2006).
- [25] Fu–Hu Liu, *Chinese Journal of Physics* **40**, 159(2002).
- [26] Powell, C.F., Fowler, F.H., and Perkins, D.H., *The Study of Elementary particles by the Photographic Method*, Pergamon Press. London, New York, Paris, Los Angeles, 474(1958).
- [27] Barkas, H., *Nuclear Research Emulsion, Vol. I, Technique and Theory* Academic Press Inc., (1963).
- [28] Abdelsalam, A., *JINR report (Dubna)* **E1–81–623** (1981).
- [29] Abdelsalam, A., Shaat, E.A., Ali–Mossa, N., Abou–Moussa, Z., Osman, O.M.,

- Rashed, N., Osman, W., Badawy, B.M., and El-Falaky, E., *J. Phys. G* **28**, 1375(2002).
- [30] Abdelsalam, A., Badawy, B.M., and El-Falaky, E., *Can. J. Phys.* **85**, 837(2007).
- [31] Bradt, H.L., and Peters, B., *Phys. Rev.* **77**, 54 (1950); **80**, 943(1950).
- [32] Adamovich, M.I., et al., *Lund University Report*, Sweden, LUIP **8904**, May(1989).
- [33] Gyulassy, M., and Kauffmann, S., K., *Phys. Rev. Lett.* **40**, 298(1978).
- [34] Hagedorn, R., *Suppl. Nuovo Cimento* **III**, 147(1965).
- [35] El-Nadi, M., Abdelsalam, A., Ali-Mossa, N., Abou-Moussa, Z., Kamel, S., Abdel-Waged, Kh., Osman, W., and Badawy, B., M., *Eur. Phys. J.* **A3**, 183(1998).
- [36] El-Nadi, M., Abdelsalam, A., Ali-Mossa, N., Abou-Moussa, Z., Abdel-Waged, Kh., Osman, W., and Badawy, B., M., *IL Nuovo Cimento A* **111**, 1243 (1998).
- [37] Angelov, N., et al., *Sov. J. Nucl. Phys.* **32**, 819(1980).
- [38] Capella, A., Casado, J.A., Pajares, C., Ramallo, A.V., and Tran Thanh Van, J., *Phys. Rev. D* **35**, 2921(1987).
- [39] Angelov, N., et al., *Sov. J. Nucl. Phys.* **33**, 552(1981).
- [40] Adamovich, M.I., et al., *Z. Phys. C* **56**, 509(1992).

التصادمات المركزية المحدثة بالأنوية الخفيفة للهدف

بدوي محمد بدوي

قسم طبيعة المفاعلات، مركز البحوث النووية، هيئة الطاقة الذرية، مصر

أجريت هذه الدراسة على تفاعلات أنوية البروتون و هيليوم - 3 و هيليوم - 4 و ليثيوم - 6 مع المستحلب النووي عند كمية تحرك 4,5 جيجا إلكترون فولت لكل نيكليون لكل وحدة سرعة ضوئية، وكانت التفاعلات المركزية هي العينة محل الاختيار لاجراء الدراسة. و قد حدد اختيار تلك العينة بالتفاعلات المصحوبة بانبعث جسيمات في الاتجاه الخلفي للتفاعل، و بغرض المقارنة قد حدد مقياس آخر لمركزية التفاعلات و هي التفاعلات المصحوبة بغياب شظايا القذيفة. و في ضوء تلك الاختيارات أجريت دراسة مسفيضة على تعددية البيونات، و كان التركيز على الأنوية الخفيفة للمستحلب النووي مقارنة بالأنوية الثقيلة. هذا و قد أتاحت الدراسة امكانية حدوث التفاعلات المركزية لأنوية المقذوفات الخفيفة مع أهداف الأنوية (CNO) في المستحلب النووي.